Comparative Evaluation of Topological and Flow-Based Seismic Resilience Metrics for Rehabilitation of Water Pipeline Systems

Zeinab Farahmandfar[1] and Kalyan R. Piratla, A.M.ASCE[2]

Abstract: Whereas the continuous functioning of water distribution pipeline systems is important during normal times, it is paramount in the event of disasters such as earthquakes that are usually followed by fire accidents. Past earthquakes resulted in severe damage to water pipelines rendering supply systems dysfunctional in a short period of time. Consequently, it is imperative to make water supply systems sufficiently resilient to seismic hazards in order to ensure better performance and faster recovery after earthquakes. There are several types of resilience metrics that were previously proposed for aiding the seismic resilience enhancement of water supply systems. This paper evaluates two such popular types, namely, topology-based and flow-based metrics, by investigating their respective capabilities in enhancing system resilience to seismic hazards. A serviceability index is defined and used to compare the performances of rehabilitated water systems for each type of resilience metric. A section of a large-scale water supply system that is vulnerable to earthquakes is leveraged in this study for the comparative performance analysis. It is found that the topology-based seismic resilience metric is on average only 80% as efficient as the flow-based metric for the studied water network. Although the flow-based metric seemed relatively superior, it suffers from the need for significant computational time. The resulting trade-off needs to be further investigated using water networks operated in multiple seismic regions. **DOI: 10.1061/(ASCE)PS.1949-1204.0000293.**

Author keywords: Infrastructure resilience; Earthquake hazard; Water pipeline rehabilitation.

Introduction

Water supply networks (WSNs) are crucial for economic prosperity and human survival. It is vital that they continue to perform despite adversities such as natural and anthropogenic hazards, random component failures, and extreme demand uncertainties. Their continuous functioning is paramount in the case of earthquakes for fighting fires that usually transpire following an earthquake. Consequently, water utility managers are increasingly showing interest in making WSNs withstand stresses, mitigate failures, minimize consequences, and recover quickly in the face of abnormalities such as earthquakes. These abilities are often together referred to as the *resilience* of the system. Several previous researchers proposed metrics to quantify resilience of WSNs in the context of seismic hazards. A common requirement in the majority of such previous studies is the simulation of WSN behavior after hazard occurrence. Broadly, the simulation models used to estimate such behavior can be categorized as topological and flow-based models.

Topological models transform the WSN's skeleton into a network graph composed of pipelines as edges and demand locations as nodes. Topological models do not truly reflect the physics-based principles of pipeline hydraulics for determining the flows and pressures, but rather base the performance prediction on the mere condition of connectivity between the source and demand nodes. On the other hand, flow-based models follow the physics-based principles of pipeline hydraulics for determining the WSN behavior. Several software tools, such as *EPANET2*, enable easy incorporation of flow-based models into resilience analysis frameworks. There is evidence in the literature that suggests contrasting results were obtained when these two types of simulation approaches were used in vulnerability or resilience analysis of infrastructure systems (Rosato et al. 2009).

If resilience metrics based on these different simulation approaches are accepted as an appropriate basis for decision making, the resulting strategies for enhancing WSN resilience could be widely contrasting. In an attempt to assess the resulting disparity, this paper comparatively evaluates topological and flow-based metrics for enhancing seismic resilience of WSNs. For a section of a real-world WSN, the two resilience metrics are used to determine the optimal resilience enhancement strategies. The resulting resilience enhancement strategies are then comparatively evaluated using a proposed serviceability index. The findings of this study reveal the relative accuracy of topological resilience metrics for usage in resilience enhancement decision making and present to the design engineer or the utility owner an insight for weighing the trade-off between the computational benefit that is often associated with the topological metrics and the resulting accuracy of their usage.

Previous Research

There has been significant focus on understanding and quantifying resilience for lifeline infrastructure systems over the past couple of decades (Matthews 2015; Piratla et al. 2016). Numerous approaches for quantifying resilience have been proposed and demonstrated with some focusing specifically on seismic resilience of water supply systems (Bruneau et al. 2003; Chang and Shinozuka 2004; Farahmandfar et al. 2015, 2016). Some studies proposed

[1]Graduate Research Assistant, Glenn Dept. of Civil Engineering, Clemson Univ., Clemson, SC 29634. E-mail: zfarahm@g.clemson.edu

[2]Assistant Professor, Glenn Dept. of Civil Engineering, Clemson Univ., Clemson, SC 29634 (corresponding author). E-mail: kpiratl@clemson.edu

Note. This manuscript was submitted on July 23, 2016; approved on June 15, 2017; published online on October 31, 2017. Discussion period open until March 31, 2018; separate discussions must be submitted for individual papers. This paper is part of the ***Journal of Pipeline Systems Engineering and Practice***, © ASCE, ISSN 1949-1190.

metrics for seismic risk and reliability (Kouli et al. 2013; Laucelli and Giustolisi 2014; Fragiadakis et al. 2013; Fragiadakis and Christodoulou 2014). The majority of previous approaches for quantifying seismic risk or resilience entail characterizing the behavior of the network that is under attack from a seismic hazard. Water networks that not only maintain maximum supply-demand connectivity but also possess adequate functional component capacity are desired when attacked by a seismic hazard. There are two categories of approaches that have been used to estimate the network performance under any type of failure: (1) topological network performance, and (2) flow-based network performance.

Studies that used topological approaches generally relied on graph theory for assessing network performance in terms of link and node connectivity under a variety of attacks (Kessler et al. 1990; Yazdani and Jeffrey 2010; Yazdani et al. 2011; Farahmandfar et al. 2017). Graphs are developed by depicting a water supply system as a set of nodes (i.e., demand locations, tanks, reservoirs, pumping stations, etc.) that are connected by pipelines as links (Farahmandfar et al. 2017). Although graph theory–based resilience metrics are distinctly meritorious for their shorter computational times, they do not truly reflect the behavior of the dynamic and nonlinear water supply systems, especially when damaged.

Studies that used flow-based approaches aimed to characterize the true behavior of water supply systems under any attack. The majority of these studies represented water supply systems using *EPANET2* models and assessed the performance by dynamically changing system statuses (Todini 2000; Prasad and Park 2004; Jayaram and Srinivasan 2008; Gay and Sinha 2012; Farahmandfar et al. 2015). Although flow-based approaches are meritorious in assessing the realistic dynamic behavior of water supply systems, they tend to be computationally challenging, especially in the case of large-scale systems, thereby limiting the extent of their performance.

Although both topology-based and flow-based modeling approaches have their respective advantages and limitations, it is vital to compare their true performance for infrastructure systems. Hines et al. (2010) compared two topological metrics with a cascading failure model using power networks and concluded that vulnerability evaluation in power networks using pure topological metrics can be misleading. Similarly, LaRocca et al. (2015) performed comparative analysis of topological and flow-based models using a test power system and concluded that topology-based measures are of limited value in analyzing the robustness of power systems under specific failure scenarios. Similar findings highlighting the limitations of topological models when compared to the flow-based ones were reported in other studies focusing on vulnerability of power (Ouyang et al. 2014a, c) and train (Ouyang et al. 2014b) infrastructure systems. Although there have been several previous studies that compared the performance merits of topology and flow-based models, none of them (i.e., to the best knowledge of the authors) used water supply systems for the comparative analysis. In an attempt to address this limitation, this paper presents a comparative analysis of topology-based and flow-based resilience metrics that are used in rehabilitation decision making with an objective of enhancing seismic resilience of water supply systems.

Research Methodology

The two-step methodology entails (1) using the topology-based and flow-based resilience metrics separately to identify optimal sets of rehabilitation (and new installation) options for a defined budget constraint, and (2) comparatively evaluating the optimal solution sets obtained from the prior step using a proposed surrogate measure of reliability, called serviceability index (SI). This section presents a brief overview of the evaluated topology and flow-based resilience metrics and describes the research methodology in greater detail.

Seismic Resilience Metrics for WSNs

The topology and flow-based resilience metrics that are evaluated in this paper are reviewed in this section.

Topology-Based Resilience Metric (TR)

The TR proposed by Farahmandfar et al. (2017) characterized seismic resilience of a WSN as a weighted function of the connectivity pattern of supply and demand nodes in conjunction with the mechanical reliability of pipelines. Their approach quantified resilience, in principle, as the summation of nodal strengths multiplied by nodal demands. Nodal strength is defined as the summation of reliabilities of all connected pipelines to that particular node. The nodal strength is multiplied with the demand at that node in order to give greater importance to nodes with higher demands. The TR metric presented by Farahmandfar et al. (2017), which is expected to be in the range from 0 to 1 in most cases, can be calculated using the following equation:

$$\mathrm{TR} = \frac{\sum_{t=1}^{td} \sum_{i=1}^{N_n} [(\sum_{j=1}^{N_i} (1 - P_{fj})) \times q_{i,t}^*]}{4 \times \sum_{t=1}^{td} \sum_{i=1}^{N_n} q_{i,t}^*} \tag{1}$$

where td = number of time steps in the demand pattern of the studied WSN; N_n = total number of nodes; N_i = degree of node i or the number of links connected to node i; P_{fj} = failure probability of link j; and $q_{i,t}^*$ = design demand of node i in time step t (L/min) (1 L = 0.26 gal.).

Flow-Based Resilience Metric (FR)

The FR proposed by Farahmandfar et al. (2015) is based on the nodal strength combined with the surplus nodal head that can be spared in cases of unusually high demands or component failures in a WSN. The buffer nodal head concept of resilience enhancement is adapted from Todini's paper that presented a resilience index suitable for the design of new WSNs (Todini 2000). Nodal demand is used in FR, similar to that in TR, to give greater importance to higher demand nodes in a WSN. FR proposed by Farahmandfar et al. (2015) can be calculated using the following equation:

$$\mathrm{FR} = \frac{\sum_{t=1}^{td} \sum_{i=1}^{N_n} [(\sum_{j=1}^{N_i} (1 - P_{fj})) q_{i,t}^* (h_{i,t} - h_{i,t}^*)]}{4 \times \sum_{t=1}^{td} \sum_{i=1}^{N_n} q_{i,t}^* h_{i,t}^*} \tag{2}$$

where $h_{i,t}$ = actual total head at node i in time step t (m) (1 m = 3.28 ft); and $h_{i,t}^*$ = minimum required total head at node i in time step t (m). The term $4 \times \sum_{t=1}^{td} \sum_{i=1}^{N_n} q_{i,t}^* h_{i,t}^*$ is added to the denominator to constrain FR value between 0 and 1 in the majority of cases.

Pipeline fragility (P_f) is used in both TR and FR to incorporate pipeline reliability, which is defined as $1 - P_f$. Assuming that the number of pipeline failures follow Poisson probability distribution (Su et al. 1987; Fragiadakis and Christodoulou 2014), pipeline fragility, defined as the probability of at least one failure on a given pipe link j, is calculated using the following equation:

$$P_{fj} = 1 - e^{-\mathrm{RR}_j * L_j} \tag{3}$$

where RR_j = repair rate (number of repairs/km/year) of pipeline j; and L_j = length of pipe link j (km) (1 km = 3,281 ft). The method presented in ALA (American Lifelines Alliance) (2001) is used in this paper to calculate repair rate (RR) of a pipeline, as described in

Farahmandfar et al. (2017). Pipeline fragility calculation leverages RRs from past earthquakes in conjunction with correction factors for pipe diameter, pipe material, and number of previous breaks (Farahmandfar et al. 2017).

Rehabilitation Planning for Seismic Resilience Enhancement

An optimization model with the objective of maximizing seismic resilience of a WSN within defined budget constraints is used to determine the optimal set of rehabilitation strategies. Seismic resilience of a WSN can be enhanced by either increasing pipelines' robustness to seismic hazards or increasing the redundancy in the system. Whereas replacement of brittle and deteriorated pipelines with flexible and new pipelines is expected to increase the robustness, installing new pipelines or increasing the capacity of existing pipelines can improve both robustness and redundancy of the system. Consequently, the decision variables in the optimization problem are a set of pipeline candidates that are shortlisted for possible replacement based on their material type and past deterioration trends, as well as possible new pipeline installations. A single-objective binary genetic algorithm is used in this study for solving the rehabilitation-planning optimization problem. The overall rehabilitation cost (C_O), which includes the cost of replacing existing pipelines as well as new installations, is calculated using the following equation:

$$C_O = \sum_{i=1}^{N_r} C_i(D_i, L_i) + \sum_{j=1}^{N_j} C_j(D_j, L_j) \tag{4}$$

where N_r = number of links that need to be replaced; $C_i(D_i, L_i)$ = cost of replacing pipe i of length L_i with diameter D_i; N_j = number of new pipelines to be added to the system; and $C_j(D_j, L_j)$ = cost of installing pipe j of length L_j and diameter D_j.

Because flexible pipelines such as those made of ductile iron and high-density polyethylene (HDPE) material have performed better during past earthquakes (Cubrinovski et al. 2014), only nonflexible pipelines are considered as candidates for replacement in this study. Also in order to accommodate the growing urban demands on WSNs, nonflexible pipelines are assumed to be replaced with flexible pipelines that are 50.8 mm (2 in.) larger in diameter. Candidate pipelines for new installations are chosen so as to connect adjacent nodes with smaller degree and greater demand. The new pipelines are assumed to be made of flexible pipe materials, and their diameter is taken as the maximum diameter of all the connecting pipe links.

Serviceability Assessment

In order to simulate the postearthquake performance of a WSN, it is necessary to predict the behavioral response of its individual components for a given magnitude of seismic hazard. Among several WSN components (such as pipelines, valves, tanks, and pumps) that continuously support its functioning, pipelines play the most significant role because they connect the supply and demand points in a WSN and often account for the majority of the capital and rehabilitation costs (Kleiner et al. 1998). Consequently, the focus in this paper is upon pipelines alone.

In response to a seismic hazard, buried pipelines may either resist the abnormal loading to continue functioning normally or fail. Pipelines fail in the form of a leak or break with varying severities. It is assumed that the number of leaks/breaks in each pipeline after an earthquake follows a Poisson distribution with the mean arrival rate equal to the estimated repair rate (RR) (Hwang et al. 1998). Upon estimating a pipeline's repair rate, a Poisson random number is generated to predict the number of damages (i.e., leaks or breaks) per 1 km (1 km = 3,281 ft) length. The generated random number is then divided into number of leaks (N_{LKS}) and number of breaks (N_{BKS}) based on the characteristics of pipe material and the seismic hazard (Hwang et al. 1998).

Typical seismic hazards of interest in the context of WSNs include: (1) transient ground deformation (TGD), which is the result of ground shaking, and (2) permanent ground deformation (PGD), which is the result of fault displacement, landslide, or liquefaction ground failures. Based on the investigation conducted by Ballantyne et al. (1990) on pipeline damage characteristics, 85% of the damages in cast iron pipes (CIP) due to TGD hazard were leaks whereas the remaining 15% were breaks. Similarly, 96% of the damages in ductile iron pipes (DIP) due to TGD hazard were leaks and 4% breaks. It was also reported that 50% of the damages due to PGD hazard were leaks and 50% breaks for all pipe materials. Using these empirical findings, the total number of leaks and breaks are calculated using the following equations:

$$N_{\mathrm{LKS}} = \mathrm{LKS}_{\mathrm{TGD}} + \mathrm{LKS}_{\mathrm{PGD}} \tag{5}$$

$$N_{\mathrm{BKS}} = \mathrm{BKS}_{\mathrm{TGD}} + \mathrm{BKS}_{\mathrm{PGD}} \tag{6}$$

where N_{LKS} and N_{BKS} = total numbers of leaks and breaks in each pipeline, respectively; $\mathrm{LKS}_{\mathrm{TGD}}$ and $\mathrm{BKS}_{\mathrm{TGD}}$ = total numbers of leaks and beaks due to TGD, respectively; and $\mathrm{LKS}_{\mathrm{PGD}}$ and $\mathrm{BKS}_{\mathrm{PGD}}$ are the total numbers of leaks and beaks due to PGD, respectively.

Upon estimating the number of leaks and breaks postearthquake, the damaged WSN is simulated using a pressure-driven demand (PDD) approach to evaluate its ability to meet the system demand. The broad approach prescribed in Hwang et al. (1998) is adapted in this study to simulate the behavior of a damaged WSN. The impacts of pipeline leaks and breaks are simulated through increasing the closely located nodal demands by amounts calculated using the orifice flow equation considering different orifice areas for leaks and breaks. The orifice areas are assumed in this study to be 3% of the pipeline cross-sectional area for a leak and 20% for a break. Subsequently, the total orifice area of a pipeline is calculated using the following equation:

$$A_T = (0.03 \times N_{\mathrm{LKS}} + 0.2 \times N_{\mathrm{BKS}}) \times A \tag{7}$$

where A_T = total orifice area of the damaged pipeline (mm^2) (1 mm^2 = 0.0015 $\mathrm{in.}^2$); and A is pipeline cross-sectional area (mm^2). The upper bound of A_T is assumed to be one cross-sectional area of the pipeline.

Orifice flows from leaks and breaks are calculated using the following equation (Tabesh et al. 2009):

$$Q_j = 84.04 \times C_d \times A_{T,j} \times P_j^{0.5} \tag{8}$$

where Q_j = discharge from the orifice of pipe j (L/min); C_d = discharge coefficient (0.8 for a hole and 0.6 for a crack shape); P_j = pressure at the orifice node (Pa) (1 Pa = 0.00014 psi), which is calculated as an average pressure of end nodes of pipe j; and $A_{T,j}$ is the total open area of pipeline j (mm^2), which is estimated using Eq. (7).

The calculated orifice flow from both leaks and breaks on each pipeline is distributed to the end nodes as additional demand for computational convenience, as illustrated in Fig. 1, using Eqs. (9) and (10)

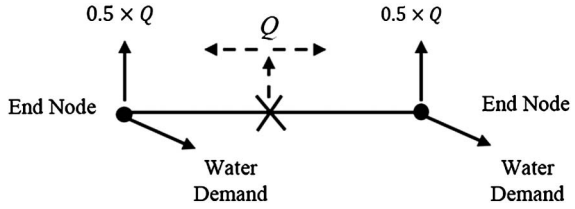

Fig. 1. Simulation approach for the impact of pipe damages

$$q_{i,t}^{\text{orifice}} = \frac{1}{2}\sum_{j=1}^{N_{p,i}} Q_j \tag{9}$$

$$q_{i,t}^{\text{required}} = q_{i,t}^{*} + q_{i,t}^{\text{orifice}} \tag{10}$$

where $q_{i,t}^{\text{orifice}}$ = total orifice flow added as additional demand at node i in time step t (L/min); $N_{p,i}$ = number of pipelines connected to node i; $q_{i,t}^{\text{required}}$ = required flow (or revised demand) at node i in time step t (L/min) after the orifice flow from leaks/breaks has been added; and $q_{i,t}^{*}$ = base demand at node i in time step t.

The damaged network is simulated using *EPANET2* in conjunction with a pressure-dependent demand (PDD) approach. *EPANET2* is a demand-driven hydraulic solver in which the demands are assumed to be fully satisfied regardless of nodal pressures. Although this assumption simplifies the computational challenge associated with hydraulic solvers, it is not appropriate for the purpose of damaged system simulation in which nodal pressures could be very low and may even become negative. Consequently, the pressure–outflow relationship is leveraged and explicitly integrated with *EPANET2* to estimate the actual flow at each node. This integrated simulation approach treats negative pressures by systematically reducing the satisfied demands in an iterative manner based on the pressure values (Liu et al. 2011). The following equation presented by Wagner et al. (1988) is used to estimate the satisfied percentage of required demand at each node

$$\text{DSR}_{i,t} = \begin{cases} 0 & \text{if } P_{i,t}^{\text{avl}} < P_{i,t}^{\min} \\ \left(\dfrac{P_{i,t}^{\text{avl}} - P_{i,t}^{\min}}{P_{i,t}^{\text{des}} - P_{i,t}^{\min}}\right)^{\frac{1}{m}} & \text{if } P_{i,t}^{\min} \le P_{i,t}^{\text{avl}} \le P_{i,t}^{\text{des}} \\ 1 & \text{if } P_{i,t}^{\text{avl}} > P_{i,t}^{\text{des}} \end{cases} \tag{11}$$

where $\text{DSR}_{i,t}$ = demand satisfaction ration of node i in time step t; $P_{i,t}^{\text{avl}}$ = actual pressure at node i in time step t (Pa); $P_{i,t}^{\min}$ = minimum required pressure at node i in time step t (Pa), below which no flow will be discharged ($P_{i,t}^{\min}$ is considered as 0 Pa in this study); $P_{i,t}^{\text{des}}$ = desired pressure at node i in time step t (Pa), below which the actual flow will be less than the required flow; and m = coefficient that is expected to range between 1.5 and 2 (Wagner et al. 1988; Gupta and Bhave 1996); a value of $m = 2$ is used in this study.

The desired pressure ($P_{i,t}^{\text{des}}$), which is dependent on the required nodal flow (or revised demand after addition of orifice flows), is calculated using the following equation (Gupta and Bhave 1996):

$$P_{i,t}^{\text{des}} = P_{i,t}^{\min} + K_{i,t}(q_{i,t}^{\text{required}})^{r} \tag{12}$$

where $K_{i,t}$ = empirical resistance factor for node i in time step t, which is considered as the ratio of nodal pressure of intact WSN ($P_{i,t}$) to the base nodal demand ($q_{i,t}^{*}$); and r = coefficient that ranges between 1.5 and 2 (Gupta and Bhave 1996); a value of $r = 1.5$ is used in this study.

A computer code is developed in this study that linked *EPANET2* software with the PDD approach using *MATLAB* programming interface to enable iterative hydraulic simulations of a damaged WSN. The developed code estimates nodal outflows based on nodal pressures using Eq. (11) after orifice flows are appropriately added to the end nodes as additional demands. The resulting nodal outflows are updated in *EPANET2* as revised demands in subsequent iterations, and this looped process, which is illustrated in Fig. 2, continues until the nodal outflows converge in successive iterations. Specifically, the iterative procedure is stopped when the maximum difference between the nodal flows in successive iterations for all nodes is less than 1% (Liu et al. 2011). When the nodal pressure is less than desired pressure and greater than minimum pressure, the nodal outflow is adjusted using the following equation:

$$q_{i,t}^{n} = q_{i,t}^{n,\text{required}} \times \frac{\text{DSR}_{i,t}^{n}}{2} + \frac{q_{i,t}^{n-1}}{2} \tag{13}$$

where n = iteration number; and $q_{i,t}^{n}$ = actual outflow at node i in time step t (L/min) in nth iteration. Half of the actual outflow from the previous iteration is added to half of the calculated nodal outflow in current iteration in order to improve the speed of convergence (Giustolisi et al. 2008). The following equation is used to estimate the portion of base nodal demand that is satisfied when nodal pressure is less than desired but greater than minimum pressure in any given iteration:

$$q_{i,t}^{\text{supplied}} = q_{i,t} \times \frac{q_{i,t}^{*}}{q_{i,t}^{\text{required}}} \tag{14}$$

where $q_{i,t}^{\text{supplied}}$ = portion of outflow that caters to the base demand at node i in time step t (L/min) (i.e., excluding the orifice flows).

Finally, the serviceability index (SI) is calculated as the ratio of summation of all nodal supplied flows to the summation of all nodal demands across all nodes and all time steps after convergence is attained, using the following equation:

$$SI = \frac{\sum_{t=1}^{td}\sum_{i=1}^{N_n} q_{i,t}^{\text{supplied}}}{\sum_{t=1}^{td}\sum_{i=1}^{N_n} q_{i,t}^{*}} \tag{15}$$

Results and Discussion

A section of the WSN that serves the Charleston Peninsula region in the state of South Carolina is slightly modified and used for comparatively evaluating the two resilience metrics. This network, hereafter referred to as CWSN, is composed of 130 pipelines that amount to approximately 12.2 km (1 km ≈ 0.62 mile) of length and has 120 demand nodes. Seventy new pipeline candidates have been identified for CWSN, as described in the methodology section, which have a combined length of 7.56 km. Fig. 3 shows the layout of CWSN. CWSN is mainly composed of cast iron (CIP) and ductile iron (DIP) pipes with diameters ranging from 101.6 to 609.6 mm. The distributions of pipe material and size for the CWSN are illustrated in Fig. 4.

Past failure information of CWSN pipelines is leveraged to integrate the effect of previous nonseismic damages with seismic vulnerability. Historical failure data for an approximately 10-year period (≈2002 to 2012) indicated that pipe segments that accounted for approximately 17% of the total CWSN length (2.15 km) have experienced at least one break. The distributions of the previous failures (or main breaks) based on pipe material and pipe diameters are shown in Fig. 5.

The Charleston region is vulnerable to seismic hazards as evidenced by the high-magnitude earthquake that occurred in the year

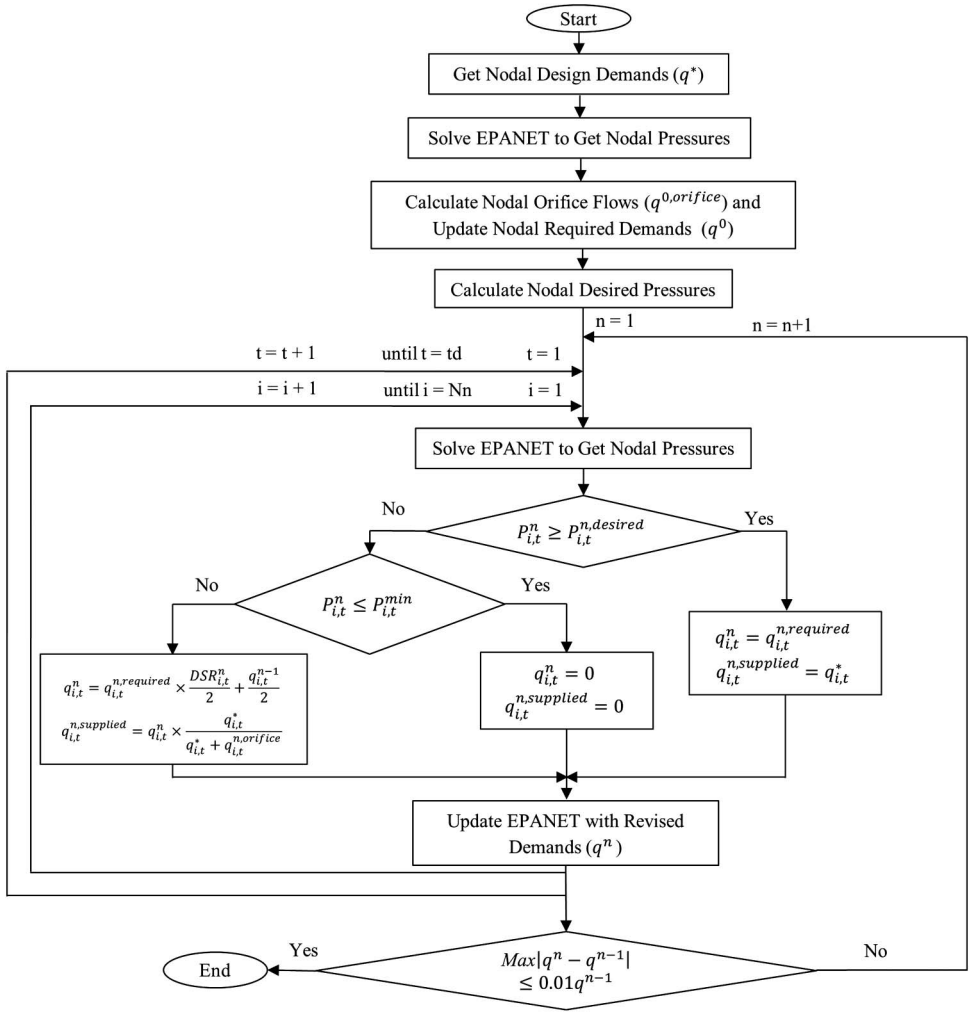

Fig. 2. Iterative hydraulic simulation for determining the damage state variables (note: i is the index of node's number; t is the index for time step; and n is the index of iteration in flow convergence loop)

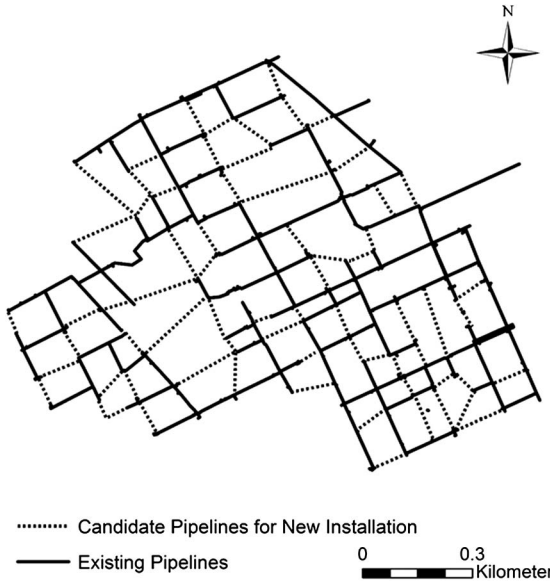

Fig. 3. Layout of the water network (CWSN) used for demonstration and evaluation of resilience metrics

1886 (Dutton 1889; Robinson and Talwani 1983; Hayati and Andrus 2008). Hayati and Andrus (2008) developed the map of liquefaction potential index (LPI) for Charleston Peninsula assuming the peak ground acceleration (PGA) of $0.3g$, which corresponds to a M_W of approximately 7. Liquefaction potential is expressed in terms of the probability that LPI will be greater than 5 ($P_{\text{LPI}>5}$), the approximate threshold for sand boil generation (Toprak and Holzer 2003). LPI was originally proposed by Iwasaki et al. (1978) for predicting the liquefaction severity at a site by considering the soil profile in the top 20 m. The liquefaction potential map of the CWSN region, presented in Fig. 6, categorizes the entire study area into three different zones with $P_{\text{LPI}>5} = 10$, 45, and 95%, respectively. Areas of $P_{\text{LPI}>5} = 95\%$ are roughly twice as likely to liquefy as areas of $P_{\text{LPI}>5} = 45\%$.

Using the $P_{\text{LPI}>5}$ values for CWSN, RRs of all pipelines are estimated using the procedure elucidated in greater detail in Farahmandfar et al. (2017). Upon calculating RRs, the pipeline fragilities are estimated using Eq. (3).

A single-objective optimization algorithm is used to identify the set of rehabilitation actions that will separately maximize the seismic resilience using topology and flow-based resilience metrics. A binary genetic algorithm with 1,000 generations per run is used with simple point crossover probability of 0.75 and a uniform mutation probability of 0.01. In order to increase the chance of finding

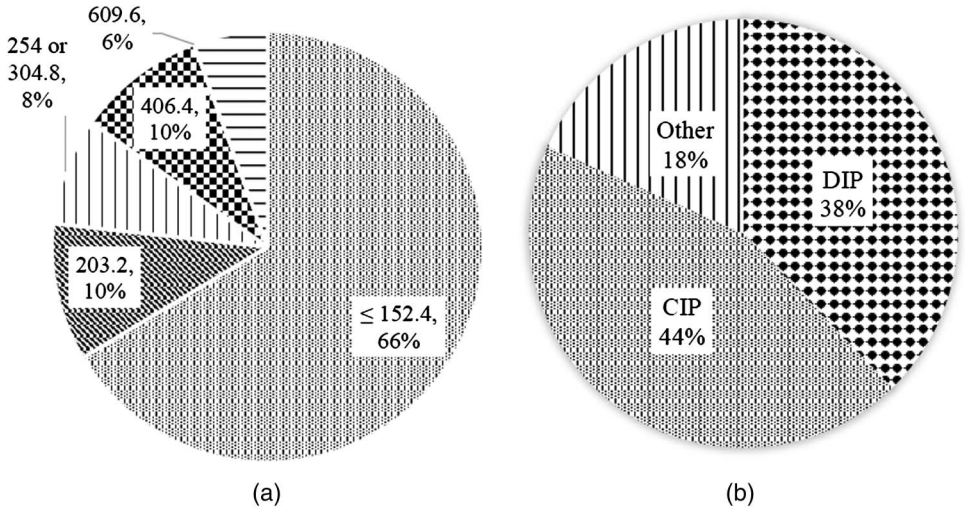

Fig. 4. CWSN characterization through distribution of pipe: (a) diameter (mm); (b) material

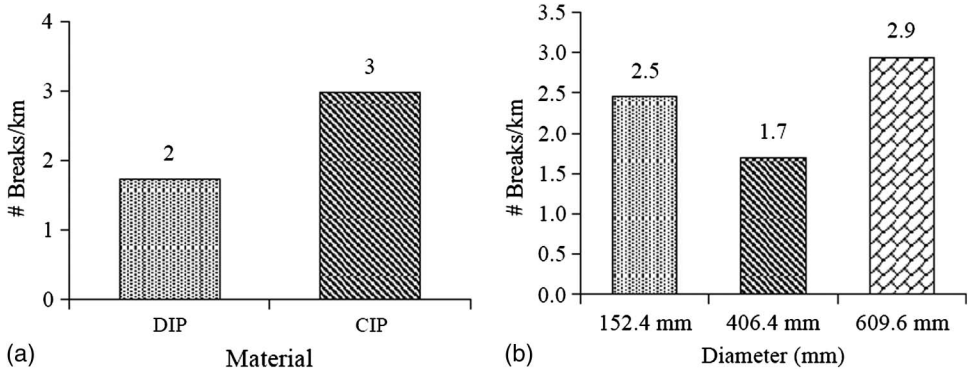

Fig. 5. Distribution of CWSN water main breaks/km by (a) pipe material; (b) pipe size

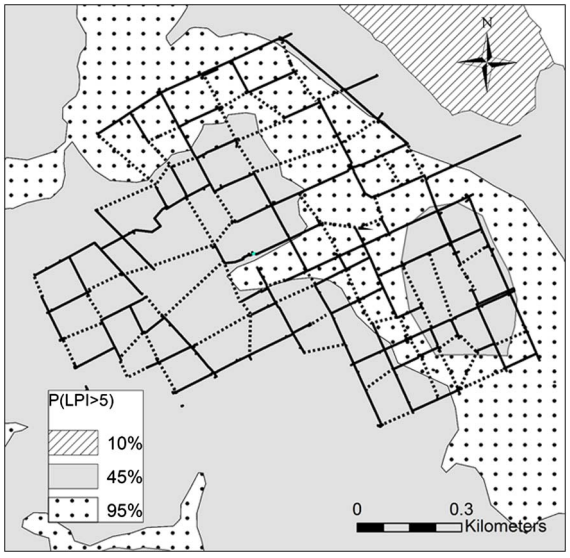

Fig. 6. CWSN layout overlaid on the liquefaction potential map of the region

the most optimal solution, five runs have been performed for each budget constraint. Rehabilitation budgets ranging from \$1 million to \$5 million in increments of \$1 million are considered to be the constraints in the optimization problem. The cost of rehabilitation is calculated using Eq. (4) assuming new installation cost of \$2.33/mm/m (\$2.33 per mm of diameter per meter of pipeline) (or \$18/in./ft) and a replacement cost of \$1.04/mm/m (\$8/in./ft). These unit costs of replacement and new installations are obtained after adjusting the low-end cost estimates presented in Boyce and Bried (1998) using a 45% inflation rate over the period 1998–2014 assuming that pipe bursting technique is used for replacement and horizontal directional drilling for new installations. The optimization algorithm is linked with the *EPANET2* toolkit in the *MATLAB* programming environment to calculate FR, whereas a *MATLAB* toolbox called Matgraph (Scheinerman 2008) is used to calculate TR. The optimization problem has been solved for a 24-h extended period for both metrics, and the run time per generation is found to be approximately 1.8 s for FR and 1.0 s for TR on an Intel i7 CPU @ 2.00 GHz processor (Santa Clara, California). As can be inferred from these computational times, TR is less computationally intense than FR. The improvements in both resilience metrics subjected to various budget constraints are shown in Fig. 7. It is clearly evident from Fig. 7 that both TR and FR increased with the budget constraint. As can be seen in Fig. 7, whereas FR has increased in a steep manner from 0.14 to 0.56 (by 300%) with the first \$1 million investment, TR has increased from 0.33 to 0.45 (by 36%). It can also be inferred that whereas TR has increased by 88% from 0.33 to 0.62, FR has increased by approximately 492% from 0.14 to 0.83 with a \$5 million investment. The steeper increment in FR compared to TR is most likely due to the fact that mathematically, FR can be increased by

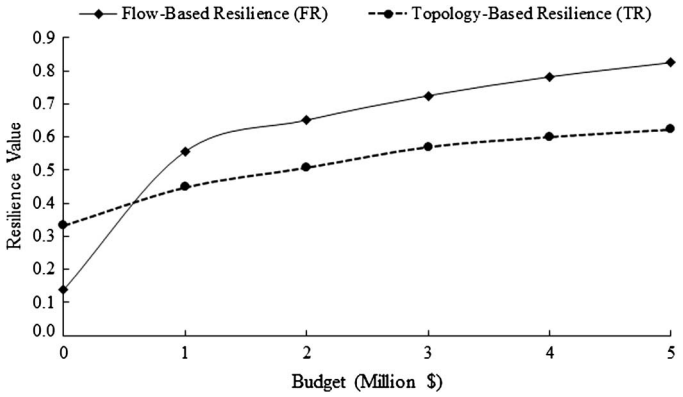

Fig. 7. Resilience versus cost trade-off for CWSN rehabilitation

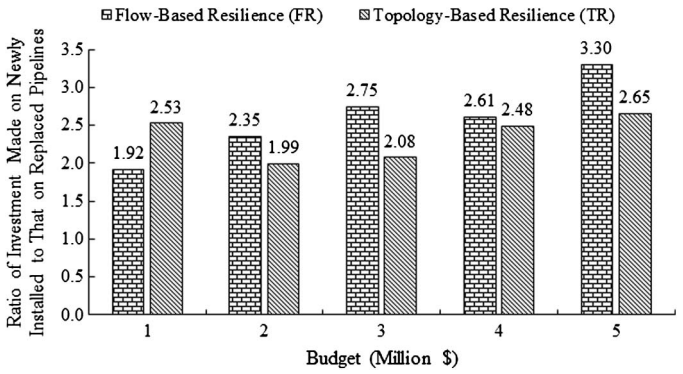

Fig. 8. Ratio of investment on newly installed to replaced pipelines of CWSN

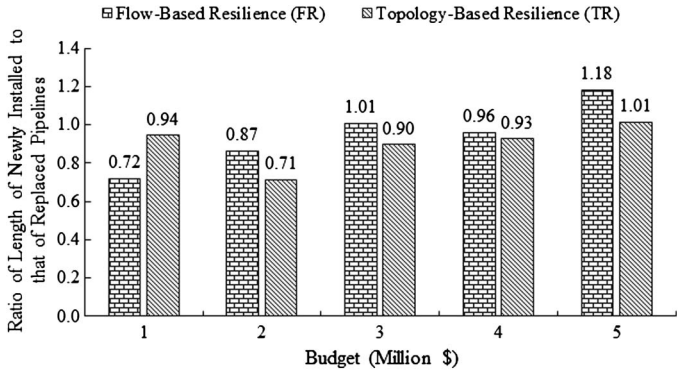

Fig. 9. Ratio of length of newly installed to replaced pipelines of CWSN

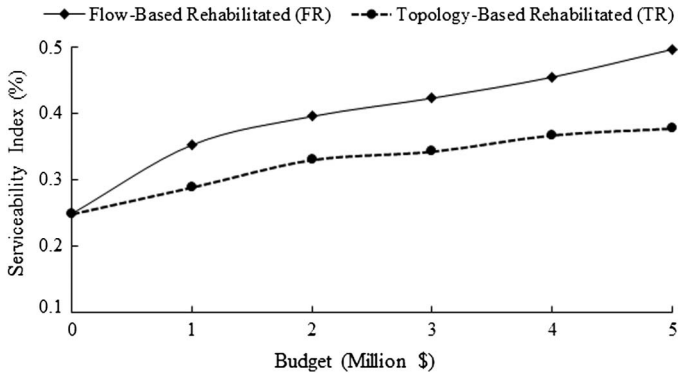

Fig. 10. Comparison of serviceability indices for CWSN in the steady-state simulation

improving both nodal pressure and nodal strength, but TR can only be increased through improved nodal strength.

Fig. 8 illustrates the ratio of investment spent on installing new pipelines to that spent on replacing existing pipelines for various budget constraints. Similarly, Fig. 9 illustrates the ratio of lengths of newly installed pipelines to replaced pipelines for various budgets. It can be inferred from Fig. 8 that approximately 71% of the investment needed to be spent on new installations on average for both TR and FR for all budgets. The greater share of investment spent on new installations despite higher unit costs ($2.33/mm/m compared to $1.04/mm/m for replacement) indicates that installing new pipelines, as considered in the rehabilitation scheme, has a greater impact on improving resilience than replacing existing pipelines. Although the amount spent on new installations is greater than replacements, it can be observed from Fig. 9 that the length of new installations is approximately equal to the length of pipeline replacements on average for all budget constraints for both TR and FR. It can also be inferred from Fig. 8 that investment made on new installations on average compared to replacements is greater in the case of FR than TR. In addition to increasing nodal pressures, installing new pipelines increases the nodal strength [i.e., $\sum_{j=1}^{N_i}(1-P_{fj})$ in Eq. (2)] through increased node degree (N_i) as well as reduced failure probability (P_{fj}). On the other hand, replacing existing pipelines increases nodal strength only through reduced failure probability. Therefore, FR, which incorporates both nodal pressure and nodal strength in its calculation, tends to increase more than TR for new installations.

It is also observed that the average nodal pressure of CWSN has increased by 62% with $5 million investment using FR, whereas it has only increased by 19% using TR. This difference is due to the fact that the FR metric is based on the hydraulic representation of the water network and it inherently incorporated buffer pressure head in its calculation. This is a key difference in the fundamentals of the two metrics that is expected to have a significant impact on the serviceability calculations presented later in this paper.

The best solutions of the optimization runs for TR and FR are evaluated based on the proposed serviceability index (SI), which is calculated using Eq. (15). The serviceability indices are estimated for both steady-state condition and a 24-h extended period assuming the hazard occurred at the beginning of the 24-h period. The SIs corresponding to the best solutions of optimization runs for various budget constraints in the steady-state condition and 24-h extended period are presented in Figs. 10 and 11, respectively. It can be observed from Figs. 10 and 11 that a positive correlation exists between SI and investment cost, and that SI trends are similar for the steady-state and extended period simulations. It can be inferred from Fig. 10 that whereas the steady-state SI of FR has increased by 96% from 0.25 to 0.49 with $5 million investment, it has increased by 48% to 0.37 using TR. It can be deduced that FR enhanced SI by 48 percentage points more than TR for a $5 million budget. Similarly, it has been observed that FR enhanced SI by 32 percentage points more than TR on average for all the budgets considered in this study. The observed superior performance of FR can be attributed to the fact that FR considers both topological and physical aspects of a WSN, unlike TR, which does not consider

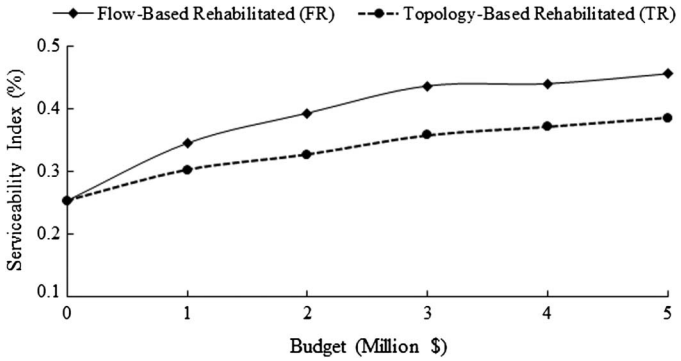

Fig. 11. Comparison of serviceability indices for CWSN in extended period simulation

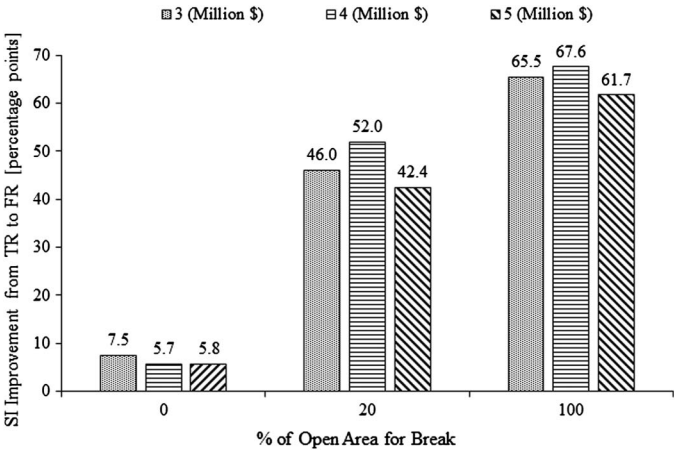

Fig. 12. Sensitivity of serviceability improvement to variation in orifice area for breaks

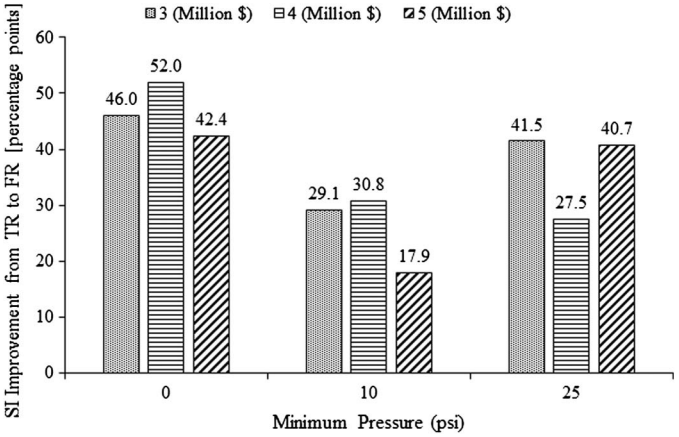

Fig. 13. Sensitivity of serviceability improvement to variation in minimum pressure values

Table 1. Parametric Assumptions and Variations for the Simulation Model

Parameter	Base value	Possible considerations	Unit
% of open area for a beak in Eq. (7)	20%	0%; 100%	%
Minimum pressure in (P^{min}) Eq. (11)	0	10; 25	psi
Empirical resistance factor (k) in Eq. (12)	$\frac{P_{i,t}}{q^*_{i,t}}$	1; 5	—
Coefficient factor (r) in Eq. (12)	1.5	2; 3	—

the physics-based aspects of pipeline systems. Although FR performed better than TR, it requires more computational time and the resulting trade-off needs to be further investigated to draw more useful conclusions.

A few parameters have been reasonably assumed, as described in the methodology section, for estimating SI values. These parametric assumptions along with a few possible variations are shown in Table 1. A one-way sensitivity analysis is conducted to evaluate the sensitivity of the findings to the variation in the parameters listed in Table 1. Figs. 12–15 present the results obtained from the sensitivity analysis in the steady-state condition.

A 20% pipeline cross-sectional area has been assumed for the orifice area of a pipeline break. This orifice area may vary depending on the stress distributions and existing weak sections in a pipeline. Because of such uncertainty with the orifice areas, the comparative performance analysis of FR and TR metrics is repeated with orifice area values of 0% (i.e., only leaks and no breaks) and 100% of the pipeline cross-sectional areas, and the results are presented in Fig. 12. It has been observed from the sensitivity analysis results that the SI value has generally decreased with increase in orifice area for both TR and FR metrics. Whereas the average SI improvement from FR to TR for the rehabilitated network over the three budget constraints is approximately 65 percentage points for orifice area of 100%, it is approximately 6 percentage points for orifice area of 0% and approximately 47 percentage points for orifice area of 20%. It can be deduced that the SI improvement of FR over TR in percentage points has generally increased with the orifice area. The observed superior performance of FR can be explained by the fact that increase in orifice area will most definitely lead to reduced system pressures and the inclusion of buffer pressure head in the calculation of FR makes it better capable of dealing with larger breaks.

Similarly, the sensitivity of SI improvement to the minimum pressure (P^{min}) parameter is evaluated. P^{min} influences the outflow at each node in the iterative hydraulic procedure adopted for calculating SI, and it is assumed to be 0 psi in this study. It can inferred from Fig. 13 that whereas FR demonstrated superior performance compared to TR for the two P^{min} values, there is not any clear trend observed between P^{min} and SI improvement. Although P^{min} is definitely expected to influence SI values, it did not seem to have a strong correlation with SI improvement from TR to FR.

Figs. 14 and 15 present the results of the sensitivity analyses for K and r coefficients, respectively, which are used in Eq. (12) to estimate the desired pressure ($P^{desired}$). The ratio of nodal pressure to nodal demand, which was found to have an average value of approximately 8, is used to estimate K in this study, and it can be observed from Fig. 14 that the resulting SI improvement from such assumption is less than when $K = 5$ and $K = 1$. The average SI improvement over the three budget constraints has almost doubled from 58 to 110 percentage points when K value is decreased from 5 to 1. A similar trend can be observed in Fig. 15 for the r coefficient where the average SI improvement has decreased from 47 to approximately 5 percentage points when the r value is doubled from 1.5 to 3. It can be inferred from Figs. 14 and 15 that SI improvement has reduced with increasing values of K and r. The considerable variation in SI improvement resulted from different values of K and r revealed the high sensitivity of SI to the desired pressure, highlighting the significance of this parameter.

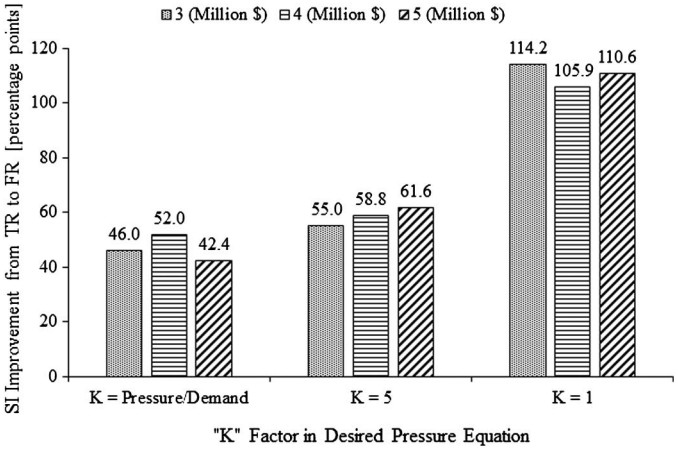

Fig. 14. Sensitivity of serviceability improvement to variation in the resistance factor (K) used in desired pressure calculation

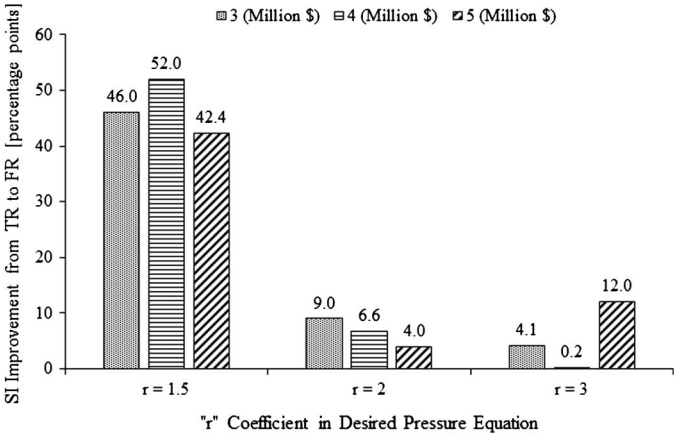

Fig. 15. Sensitivity of serviceability improvement to variation in the coefficient (r) used in desired pressure calculation

Conclusions and Recommendations

Water utility owners need optimal rehabilitation schemes that ensure water supply networks will continue to perform at their best possible level even after hazards such as earthquakes strike. Such continuous performance in the face of hazards is often referred to as the resilience of the system. Most resilience formulations proposed for WSNs in the past can be grouped into topology-based and flow-based categories. The topology-based formulations broadly capture the connectedness of the network, for example, how redundantly each demand node is connected to the supply node. Although topology-based formulations have been useful and offer a specific computational advantage, they fail to represent the physics-based phenomena of WSNs and can consequently lead to suboptimal rehabilitation schemes. On the other hand, flow-based approaches capture the true physics-based phenomena of WSNs and hence are expected to produce more accurate rehabilitation schemes, albeit at the cost of high computational time and effort. This paper presented a comparative evaluation of one topology-based and one flow-based resilience metric.

The two seismic resilience metrics are separately used to determine optimal rehabilitation strategies under various budget constraints for a section of a large WSN operating in a coastal region. The optimal set of rehabilitation strategies for each metric are comparatively evaluated using the serviceability index after simulating the behavior of the damaged WSN postearthquake hazard. The WSN behavior is simulated for both steady state condition and a 24-h period after occurrence of the earthquake hazard. The computational time required for using topology-based resilience metric is only 55% of the flow-based metric for rehabilitation planning; this benefit in computational time is expected to grow for larger networks with more complicated operational procedures. The serviceability of rehabilitated WSNs using a topology-based metric is found to be approximately 80% of those using the flow-based metric in the steady state on average for all the budget constraints; this decline in serviceability is expected to be more for larger networks with more complicated operational procedures. The serviceability of WSN in steady state as well as over an extended period postearthquake are found to be correlated and proportional to the rehabilitation budget. The sensitivity analysis of the serviceability improvement from topology-based to flow-based resilience metrics revealed a positive correlation with the orifice area of a broken pipe, no correlation with the minimum pressure parameter used in the iterative hydraulic simulation procedure, and a negative correlation with parameters K and r, which are essential for estimating the desired pressure in the iterative hydraulic simulation procedure.

The research limitations include the following: (1) the findings presented in this paper are based on analysis conducted on a smaller WSN section operating in an earthquake-prone region, and consequently the conclusions need to be further validated using additional case studies; (2) the lack of consideration of rehabilitation types such as pipe lining and cleaning in the optimization framework used in this study; (3) the lack of consideration for the type of pipeline joints that could influence the behavior of WSNs during earthquakes; and (4) the assumptions made in developing the liquefaction potential map in Fig. 6, including the assumption that older deposits are more resistant to liquefaction than younger deposits and that the open-cut pipeline installation process did not result in lower liquefaction resistance.

Acknowledgments

This research was partly supported by the National Science Foundation (NSF) under Grant No. 1638321. The views and conclusions contained in this document are those of the authors and should not be interpreted as necessarily representing the official policies, either expressed or implied, of the United States Government. The support of the NSF is greatly appreciated.

References

ALA (American Lifelines Alliance). (2001). "Seismic fragility formulations for water systems guideline and appendices." ⟨http://www.americanlifelinesalliance.com/pdf/Part_1_Guideline.pdf⟩ (Jan. 15, 2015).

Ballantyne, D. B., Berg, E., Kennedy, J., Reneau, R., and Wu, D. (1990). "Earthquake loss estimation modeling of the Seattle water system." *Technical Rep.*, Kennedy/Jenks/Chilton, Federal Way, WA.

Boyce, G. M., and Bried, E. M. (1998). "Social cost accounting for trenchless projects." *Proc., Conf. on North American No-Dig'98*, NASTT, Albuquerque, NM, 2–12.

Bruneau, M., et al. (2003). "A framework to quantitatively assess and enhance the seismic resilience of communities." *Earthquake Spectra*, 19(4), 733–752.

Chang, S. E., and Shinozuka, M. (2004). "Measuring improvements in the disaster resilience of communities." *Earthquake Spectra*, 20(3), 739–755.

Cubrinovski, M., Hughes, M., and O'Rourke, T. (2014). "Impacts of liquefaction on the potable water system of Christchurch in the 2010–2011

Canterbury (NZ) earthquakes." *J. Water Supply: Res. Technol.-Aqua*, 63(2), 95–105.
Dutton, C. E. (1889). "The Charleston earthquake of August 31, 1886." *USGS 9th Annual Rep. 1887-1888*, U.S. Geological Survey, Washington, DC, 203–528.
EPANET2 [Computer software]. EPA, Washington, DC.
Farahmandfar, Z, Piratla, K. R., and Andrus, R. D. (2015). "Flow-based modeling for enhancing seismic resilience of water supply networks." *Pipelines 2015*, ASCE, Reston, VA, 756–765.
Farahmandfar, Z., Piratla, K. R., and Andrus, R. D. (2017). "Resilience evaluation of water supply networks against seismic hazards." *J. Pipeline Syst. Eng. Pract.*, 10.1061/(ASCE)PS.1949-1204.0000251, 04016014.
Fragiadakis, M., and Christodoulou, S. E. (2014). "Seismic reliability assessment of urban water networks." *Earthquake Eng. Struct. Dyn.*, 43(3), 357–374.
Fragiadakis, M., Christodoulou, S. E., and Vamvatsikos, D. (2013). "Reliability assessment of urban water distribution networks under seismic loads." *Water Resour. Manage.*, 27(10), 3739–3764.
Gay, L., and Sinha, S. (2012). "Novel resilience assessment methodology for water distribution systems." *Pipelines 2012@sInnovations in Design, Construction, Operations, and Maintenance, Doing More with Less*, ASCE, Reston, VA, 61–69.
Giustolisi, O., Savic, D., and Kapelan, Z. (2008). "Pressure-driven demand and leakage simulation for water distribution networks." *J. Hydraul. Eng.*, 10.1061/(ASCE)0733-9429(2008)134:5(626), 626–635.
Gupta, R., and Bhave, P. R. (1996). "Comparison of methods for predicting deficient network performance." *J. Water Resour. Plann. Manage.*, 10.1061/(ASCE)0733-9496(1996)122:3(214), 214–217.
Hayati, H., and Andrus, R. D. (2008). "Liquefaction potential map of Charleston, South Carolina based on the 1886 earthquake." *J. Geotech. Geoenviron. Eng.*, 10.1061/(ASCE)1090-0241(2008)134:6(815), 815–828.
Hines, P., Cotilla-Sanchez, E., and Blumsack, S. (2010). "Do topological models provide good information about electricity infrastructure vulnerability?" *Chaos: Interdiscip. J. Nonlinear Sci.*, 20(3), 033122.
Hwang, H. H., Lin, H., and Shinozuka, M. (1998). "Seismic performance assessment of water delivery systems." *J. Infrastruct. Syst.*, 10.1061/(ASCE)1076-0342(1998)4:3(118), 118–125.
Iwasaki, T., Tatsuoka, F., Tokida, K. I., and Yasuda, S. (1978). "A practical method for assessing soil liquefaction potential based on case studies at various sites in Japan." *Proc., 2nd Int. Conf. on Microzonation*, National Science Foundation, Washington, DC, 885–896.
Jayaram, N., and Srinivasan, K. (2008). "Performance-based optimal design and rehabilitation of water distribution networks using life cycle costing." *Water Resour. Res.*, 44(1), W01417.
Kessler, A., Ormsbee, L., and Shamir, U. (1990). "A methodology for least-cost design of invulnerable water distribution networks." *Civ. Eng. Syst.*, 7(1), 20–28.
Kleiner, Y., Adams, B. J., and Rogers, J. S. (1998). "Long-term planning methodology for water distribution system rehabilitation." *Water Resour. Res.*, 34(8), 2039–2051.
Kouli, M., Papadopoulos, I., and Vallianatos, F. (2013). "Preliminary GIS based analysis of seismic risk in water pipeline lifeline system in urban infrastructure of Chania (Crete)." *1st Int. Conf. on Remote Sensing and Geoinformation of Environment*, International Society for Optics and Photonics, Bellingham, WA, 885–896.
LaRocca, S., Johansson, J., Hassel, H., and Guikema, S. (2015). "Topological performance measures as surrogates for physical flow models for risk and vulnerability analysis for electric power systems." *Risk Anal.*, 35(4), 608–623.
Laucelli, D., and Giustolisi, O. (2014). "Vulnerability assessment of water distribution networks under seismic actions." *J. Water Resour. Plann. Manage.*, 10.1061/(ASCE)WR.1943-5452.0000478, 04014082.
Liu, J., Yu, G., and Savic, D. (2011). "Deficient-network simulation considering pressure-dependent demand." *Sustainable Solutions for Water, Sewer, Gas, and Oil Pipelines (ICPTT 2011)*, ASCE, Reston, VA, 886–900.
MATLAB [Computer software]. MathWorks, Natick, MA.
Matthews, J. C. (2015). "Disaster resilience of critical water infrastructure systems." *J. Struct. Eng.*, 10.1061/(ASCE)ST.1943-541X.0001341, C6015001.
Ouyang, M., Pan, Z., Hong, L., and Zhao, L. (2014a). "Correlation analysis of different vulnerability metrics on power grids." *Physica A*, 396, 204–211.
Ouyang, M., Zhao, L., Hong, L., and Pan, Z. (2014b). "Comparisons of complex network based models and real train flow model to analyze Chinese railway vulnerability." *Reliab. Eng. Syst. Saf.*, 123, 38–46.
Ouyang, M., Zhao, L., Pan, Z., and Hong, L. (2014c). "Comparisons of complex network based models and direct current power flow model to analyze power grid vulnerability under intentional attacks." *Physica A*, 403, 45–53.
Piratla, K. R., Matthews, J. C., and Farahmandfar, Z. (2016). "The role of resilience in rehabilitation planning of water pipeline systems." *ASCE Pipelines*, ASCE, Reston, VA, 1856–1864.
Prasad, T. D., and Park, N. S. (2004). "Multiobjective genetic algorithms for design of water distribution networks." *J. Water Resour. Plann. Manage.*, 10.1061/(ASCE)0733-9496(2004)130:1(73), 73–82.
Robinson, A., and Talwani, P. (1983). "Building damage at Charleston, South Carolina, associated with the 1886 earthquake." *Bull. Seismol. Soc. Am.*, 73(2), 633–652.
Rosato, V., Issacharoff, L., Gianese, G., and Bologna, S. (2009). "Influence of the topology on the power flux of the Italian high-voltage electrical network." ArXiv e-prints arXiv:0909.1664v1.
Scheinerman, E. R. (2008). "Matgraph: A MATLAB toolbox for graph theory." Johns Hopkins Univ., Baltimore, 1–7.
Su, Y. C., Mays, L. W., Duan, N., and Lansey, K. E. (1987). "Reliability based optimization model for water distribution systems." *J. Hydraul. Eng.*, 10.1061/(ASCE)0733-9429(1987)113:12(1539), 1539–1556.
Tabesh, M., Yekta, A. A., and Burrows, R. (2009). "An integrated model to evaluate losses in water distribution systems." *J. Water Resour. Plann. Mange.*, 23(3), 477–492.
Todini, E. (2000). "Looped water distribution networks design using a resilience index based heuristic approach." *Urban Water*, 2(2), 115–122.
Toprak, S., and Holzer, T. L. (2003). "Liquefaction potential index: Field assessment." *J. Geotech. Geoenviron. Eng.*, 10.1061/(ASCE)1090-0241(2003)129:4(315), 315–322.
Wagner, J. M., Shamir, U., and Marks, D. H. (1988). "Water distribution reliability: Simulation methods." *J. Water Resour. Plann. Mange.*, 114(3), 276–294.
Yazdani, A., and Jeffrey, P. (2010). "A complex network approach to robustness and vulnerability of spatially organized water distribution networks." *Physics*, ArXiv arXiv:1008.1770.
Yazdani, A., Otoo, R. A., and Jeffrey, P. (2011). "Resilience enhancing expansion strategies for water distribution systems: A network theory approach." *Environ. Modell. Software*, 26(12), 1574–1582.